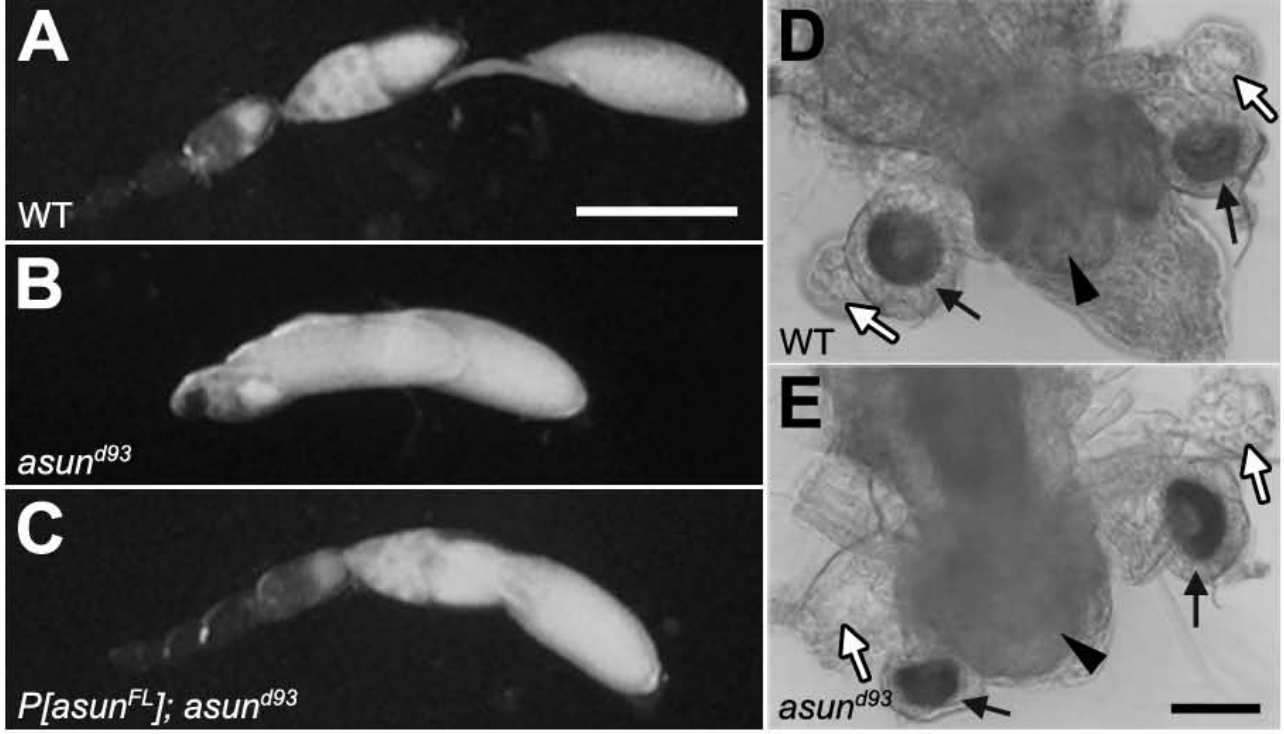

Figure S1. Defective ovulation with normal reproductive glands in *asun*^{d93} females. (A-C) Micrographs of ovarioles isolated from fattened females of indicated genotypes. Germaria, left; mature eggs, right. Wild-type and rescued *asun*^{d93} ovarioles (A and C, respectively) contain a linear sequence of egg chambers of increasing developmental stages. *asun*^{d93} ovarioles (B) contain juxtaposed early and mature egg chambers with intermediate stages missing. Scale bar, 500 μm. (D,E) Phase-contrast images of female reproductive glands from wild-type and *asun*^{d93} females. As in wild type (D), a seminal receptacle (black arrowhead), a pair of spermathecae (black arrows), and a pair of parovaria (white arrows) are present in *asun*^{d93} (E) females. Scale bar, 200 μm.

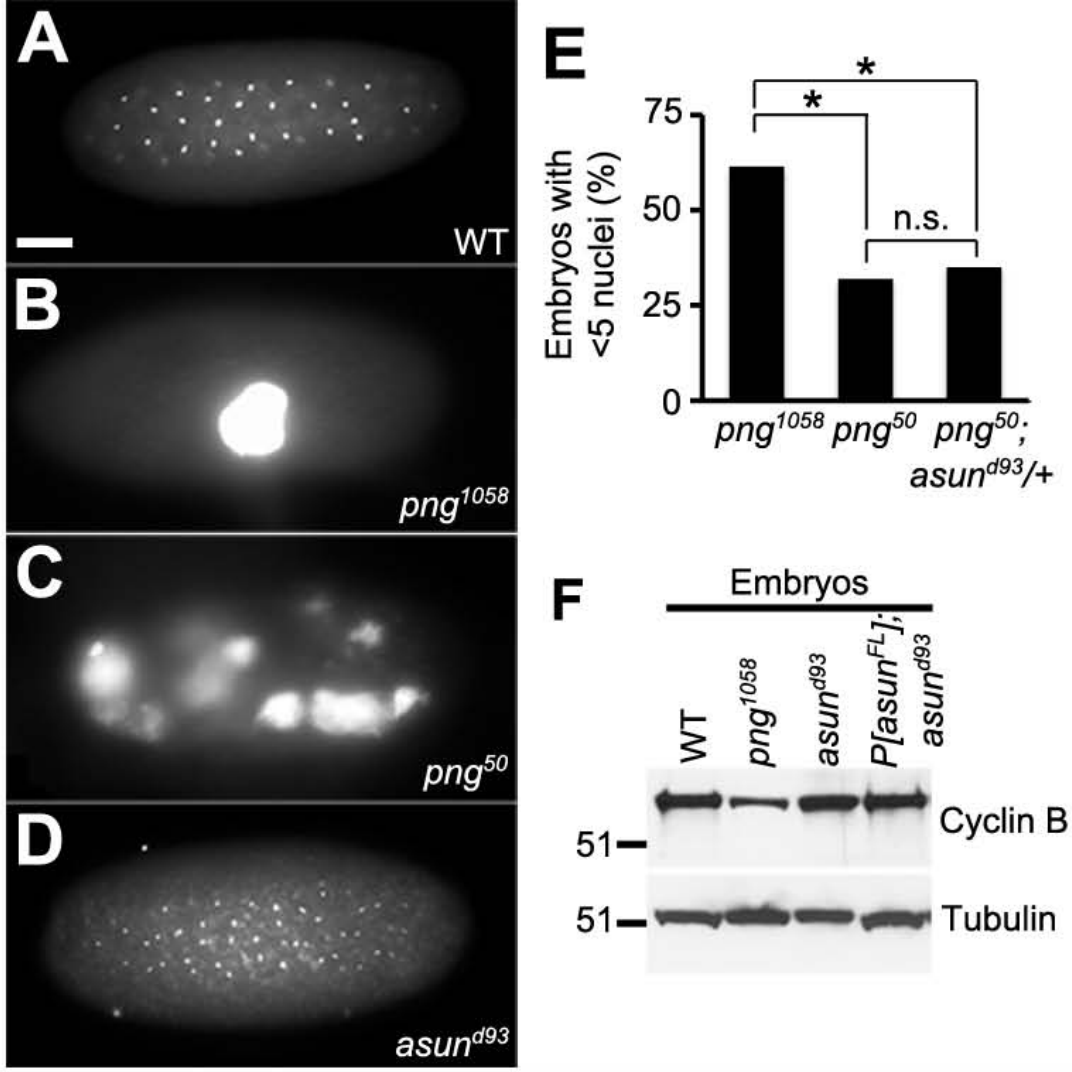

Figure S2. *asun*^{d93}-derived embryos do not exhibit the giant nuclei phenotype. (A-D) DNA-stained embryos (0-2 hour) from wild-type, *png*, or *asun*^{d93} females. Embryos from wild-type (A) and *asun*^{d93} (D) females exhibit a normal DNA staining pattern, unlike the giant nuclei phenotype observed in the strong (B) and weak (C) alleles of *png*. Scale bar, 50 µm. (E) Quantification of embryos (0-2 hour) containing fewer than 5 nuclei (>200 embryos scored per genotype). Asterisks, $p<0.0001$; n.s., not significant. (F) Immunoblot showing wild-type levels of Cyclin B in extracts of embryos (0-2 hour) from *asun*^{d93} and rescued *asun*^{d93} females. Cyclin B levels are reduced in *png*^{1058}-derived embryos. Tubulin, loading control.

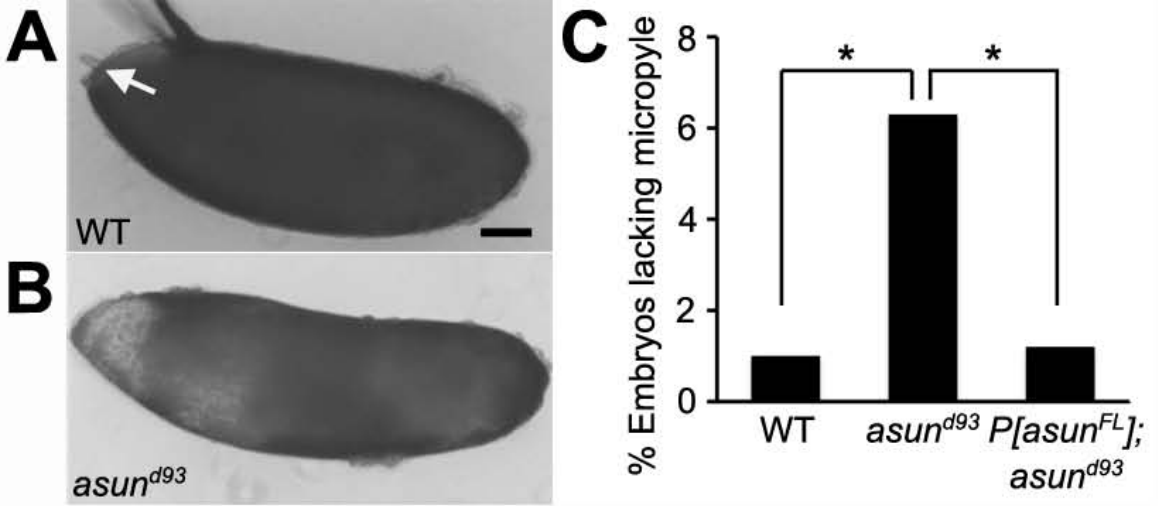

Figure S3. Lack of a micropyle is a low-penetrance phenotype of *asun*^{d93}-derived embryos. (A,B) Phase-contrast images of whole embryos derived from wild-type (A) or *asun*^{d93} (B) females. Anterior, left; dorsal, top. The micropyle (white arrow) is occasionally absent in embryos derived from *asun*^{d93} females. Scale bar, 100 μm. (C) Quantification of wild-type and *asun*^{d93}-derived embryos lacking a micropyle (>200 embryos scored per genotype). Asterisks, $p<0.005$.

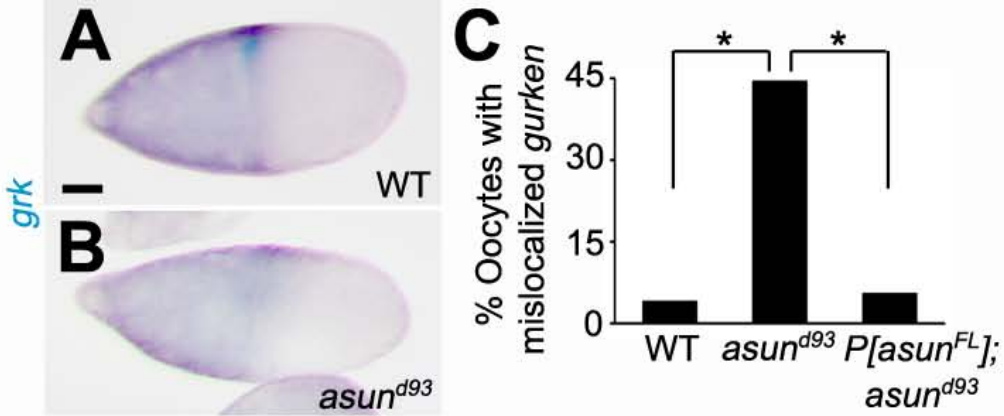

Figure S4. Diffuse localization of *grk* transcripts in *asun*^{d93} oocytes. (A-B) Enzymatic in situ hybridization of stage 10 egg chambers using *grk* probe (dorsal, top; anterior, left). *grk* mRNA localization is tightly restricted to the anterior-dorsal region of the oocyte in wild-type egg chambers (A). In *asun*^{d93} egg chambers, *grk* transcripts are more diffusely localized throughout the anterior oocyte (B). Scale bars, 50 μm. (C) Quantification of diffusely localized *gurken* transcripts in wild-type, *asun*^{d93}, and rescued *asun*^{d93} oocytes (>100 chambers scored per genotype) by enzymatic in situ hybridization. Asterisks, $p<0.0001$.

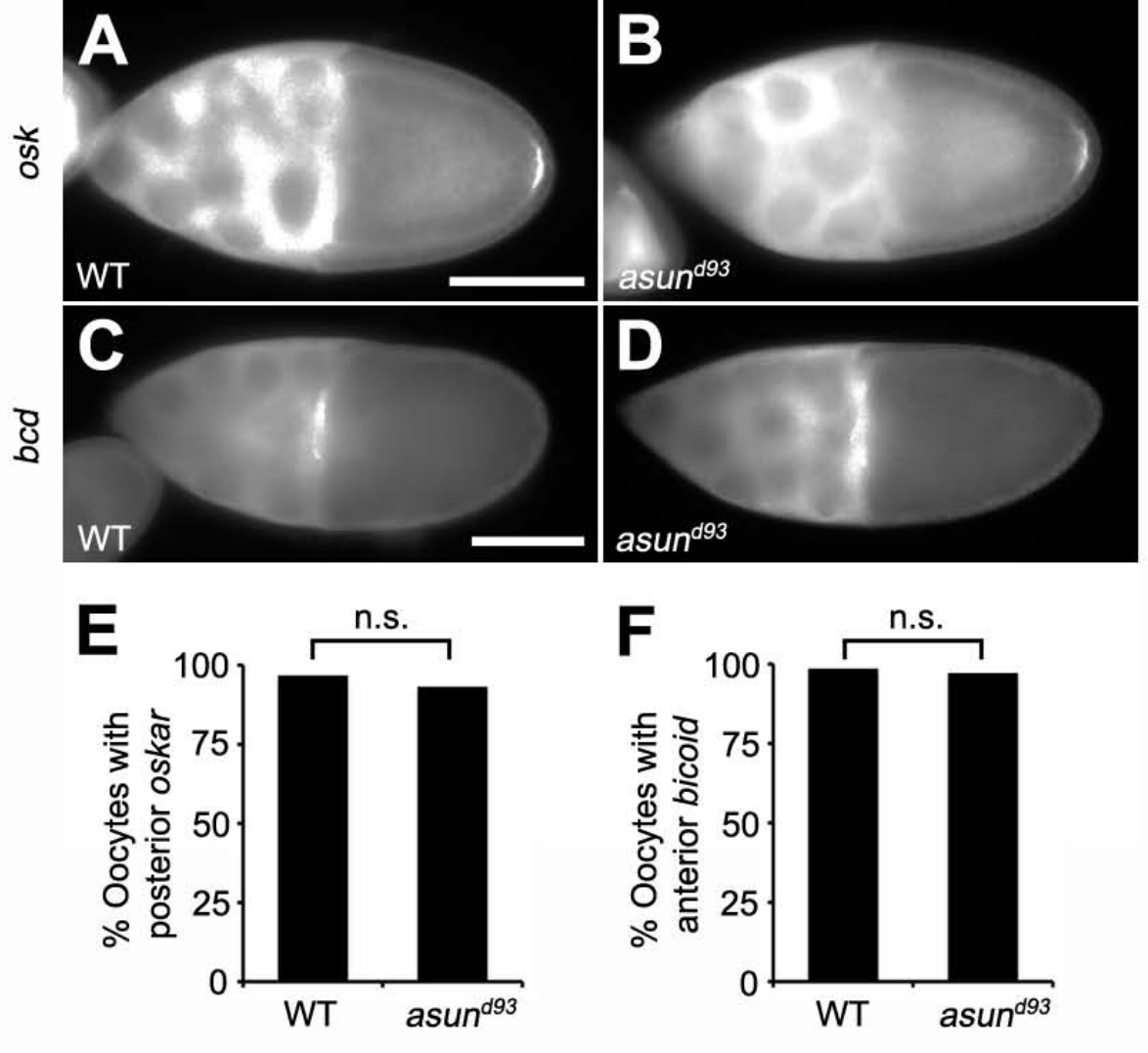

Figure S5. Wild-type localizations of *osk* and *bcd* transcripts in *asun*^{d93} oocytes. Fluorescent in situ hybridizations of stage 10 egg chambers using *osk* and *bcd* probes (dorsal, up; anterior, left). (A,B) Representative images showing normal localization of *osk* mRNA to the posterior pole of the oocyte in wild-type (A) and *asun*^{d93} (B) egg chambers. (C,D) Representative images showing normal localization of *bcd* mRNA to the anterior region of the oocyte in wild-type (C) and *asun*^{d93} (D) egg chambers. Scale bars, 100 µm. (E,F) Quantification of properly localized *osk* (E) and *bcd* (F) transcripts in wild-type and *asun*^{d93} egg oocytes (>100 chambers scored per sample). n.s., not significant.

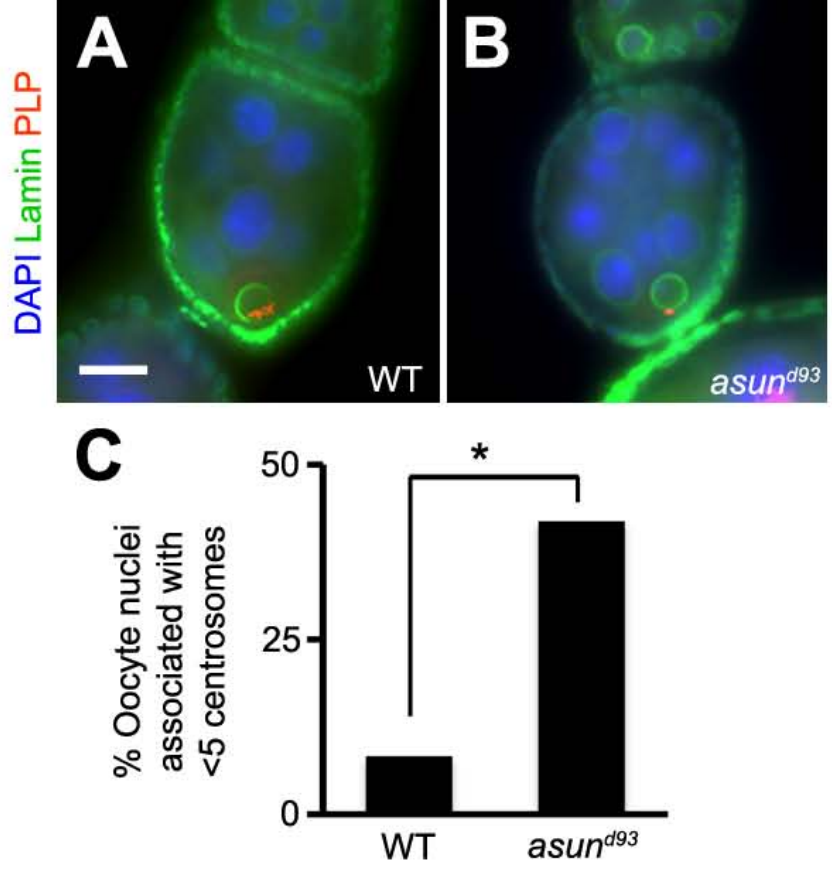

Figure S6. Reduced centrosome number in *asun*^{d93} oocytes. (A,B) Stage 5 egg chambers stained for lamin (green; NE marker), PLP (red; centriole marker), and DNA (blue). Anterior, top; dorsal, right. Fewer centrosomes are associated with the oocyte nucleus in *asun*^{d93} (B) than wild-type (A) egg chambers. Scale bar, 20 μm. (C) Quantification of reduced centrosome number in wild-type and *asun*^{d93} ovaries (>40 chambers scored per genotype). Asterisk, $p<0.0001$.

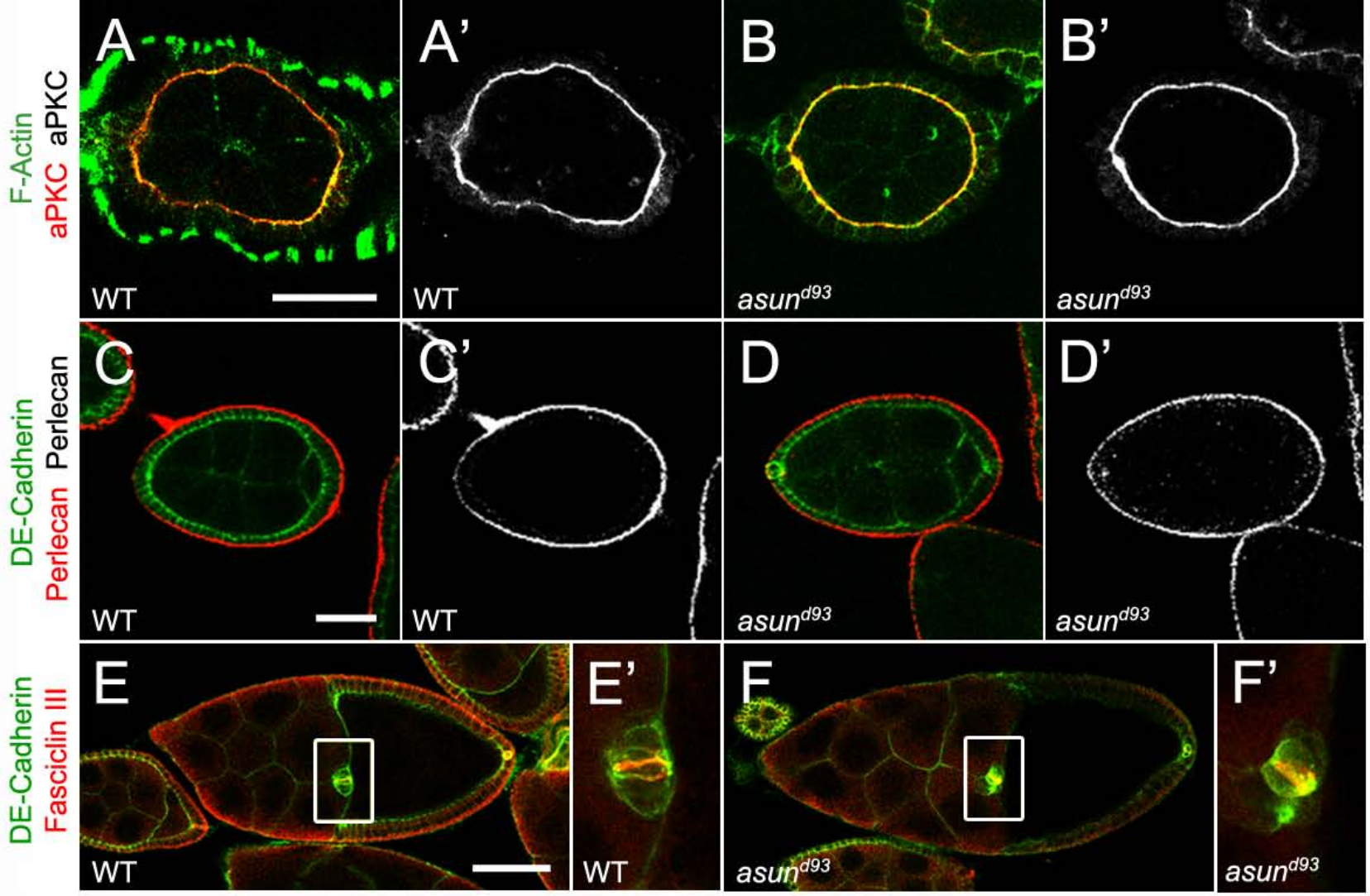

Figure S7. Normal apical-basal polarity of follicle cells and migration of border cells in *asun*^{d93} egg chambers. (A-B') Stage 4 egg chambers stained for F-Actin (green; cell membrane marker) and aPKC (red; grayscale in A' and B'; marker for apical surface of follicle cells). aPKC protein localizes to the apical surface of the epithelial follicle cells in wild-type and *asun*^{d93} egg chambers. Scale bar, 20 μm. (C-D') Stage 6 egg chambers stained for DE-Cadherin (green; cell membrane marker) and expressing GFP-tagged Perlecan protein (red; grayscale in C' and D'; marker for basal surface of follicle cells). Perlecan localizes to the basal surface of the epithelial follicle cells in wild-type and *asun*^{d93} egg chambers. Scale bar, 20 μm. (E-F') Stage 10 egg chambers stained for DE-Cadherin (green; cell membrane marker) and Fasciclin III (red; marker for polar cells). The migratory border cells, including the polar cells (enlarged within E' and F'), have migrated to the border between the oocyte and the nurse cells in stage 10 wild-type and *asun*^{d93} egg chambers. Scale bar, 50 μm. Anterior, left; dorsal, top.